

Structural Details of a Fowl Feather Elucidated by Using Polarized Raman Microspectroscopy

Yoshiko Yokote,*[1] Yoshiko Kubo,[2] Rieko Takahashi,[1] Teruki Ikeda,[2] Kiso Akahane,[1] and Masamichi Tsuboi[3]

[1]Department of Chemistry, Faculty of Science, Josai University, Sakado 350-0290

[2]JASCO, Hachioji, Tokyo 193-0943

[3]Department of Science and Engineering, Iwaki-Meisei University, 5-5-1 Chuodai-Iino, Iwaki 970-8551

Received August 14, 2006; E-mail: yokote@josai.ac.jp

Raman spectra of undeuterated and deuterated rachis from a fowl feather was observed with 488 nm excitation in the 400–1800 cm^{-1} region. Fowl feather rachis and barbs were subjected to a polarized Raman microscopic examination with excitation at 785 nm. From the observed frequencies, intensities, and scattering anisotropies of the 20 Raman bands, and on the basis of known Raman tensors of the 10 localized molecular vibrations, conformations, and orientations of the polypeptide main chains, tyrosine, phenylalanine, tryptophan residues, and disulfide linkages of the protein molecules in the feather were elucidated.

We have been engaged for many years in chemical analysis of avian feathers. Proteins involved in feathers are insoluble in usual protein solvents, but they can be solubilized by cleaving the disulfide linkage. The extract, which constitutes about 85% of the mass of feather, has been found to consist of a mixture of many closely related polypeptide chains.[1–3] We have established a systematic separation method for such mixtures and for primary structures of single polypeptide chains from feather barbs (Fig. 1) of fowls, ducks, and pigeons.[3–7]

We are now attempting to extend this work to analyze physically the avian feathers. One promising method is considered to be Raman spectroscopy, because a number of examples of Raman spectroscopic examinations of proteins are already known.[8–16] This is the first report of our work along this line. Here, we show that an in situ Raman spectroscopic measurements of fowl feather is possible. The fluorescence disturbance could be avoided, and average conformations and orientations of peptide groups and several amino acid side chains were determined.

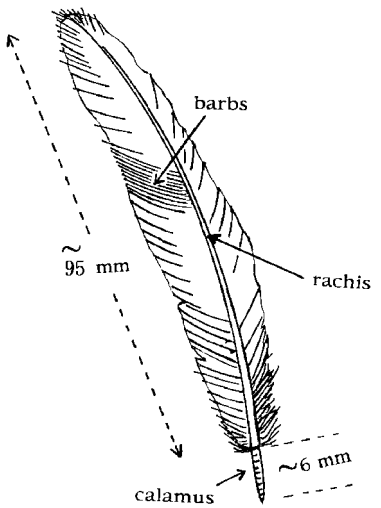

Fig. 1. Rachis, barbs, and calamus parts of a feather.

Experimental

Sample Preparation. A white body feather from a fowl was washed in a dilute non-ionic detergent solution, rinsed repeatedly in pure water, air-dried and degreased by soaking in fresh dry acetone, refluxed with dry ether for two or more days to remove fluorescent impurity, and then air-dried again. The intensity of the fluorescence from impurities was found to decrease gradually when the feather sample was degreased repeatedly by soaking in solvents that dissolve fat. The dry feather was separated into morphologically distinct parts, rachis, barbs, and calamus, according to the method described by Schroeder et al.[17] The rachis and barb parts (Fig. 1) were used for our present analysis.

Deuteration. About 0.1 g of the dry rachis was immersed in 5.0 mL of D_2O (99.75%, from E. Merck). The sample for deuteration was evacuated, sealed, and then allowed to stand for 7 days at 40 °C in D_2O. After 7 days of deuteration, the sample was lyophilized in vacuo.

Amino-Acid Analysis. Feather samples were hydrolyzed with 6 M (1 M = 1 mol dm^{-3}) HCl containing 3% sulfanylacetic acid in vacuo at 110 °C for 24, 48, or 72 h. The hydrolyzates were subjected to JEOL JLC-300 amino acid analyzer (Table 1). Tryptophan contents were determined separately by the method described by Penke et al.[18]

Raman Spectroscopic Measurements. Raman spectra of feather rachis were obtained on a Jasco NR-11 Raman Spectrometer with 488 nm excitation (Coherent Innova 70 Ar^+ laser, 70 mW). A slit width corresponding to 6 cm^{-1} and a 90° scattering geometry was used. Each sample was irradiated with a low power laser light before measurement for about 2 h in order to reduce the fluorescence, which came from a small amount of fluorescent material that still remained. The peak wavenumbers of sharp Raman

Published on the web June 13, 2007; doi:10.1246/bcsj.80.1148

Table 1. Amino Acid Analyses of Rachis and Barbs Parts and CM-Protein Fractions from Whole Feather of a Fowl

Amino acid	Residues per 100 residues			
	Rachis part	Barbs part	CM-Soluble portion	CM-Insoluble portion
Aspartic acid	6.0	6.0	5.0	8.5
Threonine	4.7	5.0	4.5	6.2
Serine	13.2	14.7	14.6	8.1
Glutamic acid	7.9	7.6	7.7	11.3
Glycine	13.0	11.5	11.9	8.5
Alanine	8.0	5.0	5.3	5.8
CM-Cysteine	8.0	8.1	8.3	8.7
Valine	7.4	7.7	9.1	7.3
Methionine	0.0	0.3	0.0	1.2
Isoleucine	3.2	4.3	4.9	4.0
Leucine	8.1	7.0	7.0	6.8
Tyrosine	1.3	1.4	1.2	2.8
Phenylalanine	3.4	3.6	3.5	2.4
Histidine	0.2	0.3	0.0	1.4
Lysine	0.4	0.6	0.4	3.7
Arginine	4.2	4.7	4.8	4.2
Proline	10.6	11.7	11.8	7.5
Tryptophan	0.4	0.5	0.0	1.6

bands were reproducible to within $\pm 1\,cm^{-1}$.

Polarized Raman Microspectroscopy. To obtain the Raman spectra, the samples were excited at 785 nm with 70 mW of radiant power from a solid-state diode laser (Torsano Star Bright 785) that was coupled to a Jasco NRS 3200 Raman microscope. Each spectrum displayed in the figures is the average of 100 exposures of 15 s each. Raman wavenumbers were calibrated using the emission lines from a neon lamp and $459\,cm^{-1}$ band of liquid CCl_4. The laser beam was directed into the 100× objective and into the rachis. The back-scattered (180°) Raman photons were collected with the same objective, passed through a polarizing analyzer, directed onto the slit of the spectrometer, and detected by charge-coupled device detector optimized for the near-infrared region. The incident laser beam, propagating in the ***a*** direction, was adjusted so that its direction of polarization (***b***) was perpendicular to the rachis axis (***c***). The polarizing analyzer was adjusted to either the same (***b***) or the perpendicular direction (***c***).

The polarized Raman intensities (***Icc*** and ***Icb***) were measured by maintaining the rachis in a fixed orientation and rotating the polarizing analyzer. These intensities correspond to the rachis tensor components, ***cc*** and ***cb***, respectively, where ***c*** is the rachis axis and ***b*** is perpendicular to ***c***. The notation ***Icc*** signifies that the electric vectors of both the excitation and scattered radiation are along ***c***; similarly, ***Icb*** signifies that excitation and scattered electric vectors are along ***b*** and ***c***, respectively. Subsequent rotation of the fiber by 90° on the microscope platform allowed ***Ibb*** and ***Ibc*** to be measured in succession using the same procedure as described earlier. If the laser beam is precisely focused on the same portion of the sample throughout this protocol, then we expect ***Icb*** = ***Ibc***. This was found to be the case in every experimental protocol.

Both of feather rachis and barbs were subjected to the polarized Raman examination. The results are similar to each other, and no significant differences were found.

Results and Discussion

Preliminary Analysis. Raman spectra of feather rachis obtained with 488 nm excitation and without a polarizer are shown in Fig. 2. Polarized Raman spectra of feather rachis excited at 785 nm are shown in Fig. 3. Observed frequencies of the Raman bands are listed in Table 2. All of these spectra were observed for a fowl feather rachis (or barb) itself (solid state) before any chemical or physical action was made on it. Such a solid material is now known to consist of proteins, and their amino-acid residue compositions are listed in Table 1. On the basis of such a chemical analysis, and on the basis of the results of previous Raman studies of proteins, a possible assignment of the each Raman band is given in Table 2.

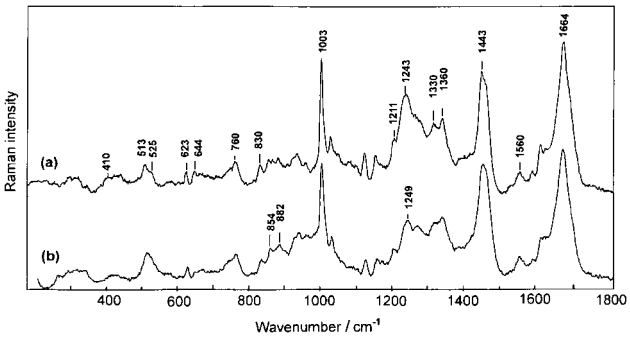

Fig. 2. Ramam spectra of native (a) and deuterated (b) feather rachis in the solid states excited at 488 nm.

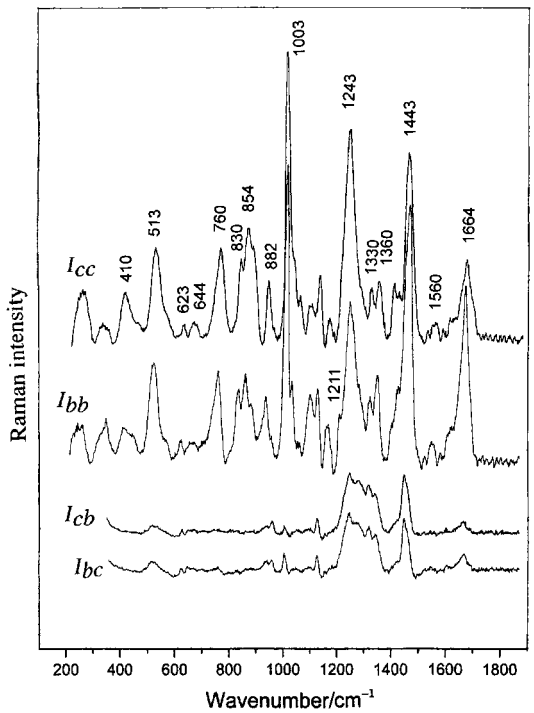

Fig. 3. From top to bottom: Polarized ***Icc***, ***Ibb***, ***Icb***, and ***Ibc*** Raman spectra (200–1800 cm^{-1}) of fowl feather rachis, excited at 785 nm.

The proteins in a feather are insoluble in normal protein solvents, and this property is considered to be largely due to cross-linking of cystine residues. Soluble proteins can be prepared by reduction and alkylation of the disulfide bonds.[19] We have previously prepared *S*-carboxymethyl (CM) proteins

Table 2. Raman Bands of Native and Deuterated Rachis from Fowl Feathers

Native/cm^{-1}	Deuterated/cm^{-1}	Assignments
410 m	410 m	Tyr
513 m	517 m	S–S stretching
525 w		S–S stretching
623 w	623 w	Phe
644 w	644 vw	Tyr
760 m	760 m	Trp
830 w	830 w	Tyr
854 w	854 w	Tyr
882 w	882 w	Trp
936 w	936 w	
	932 w	amide III′
	962 w	amide III′
1003 s	1003 s	Phe
1033 w	1033 w	Phe
1129 w	1129 w	
1159 w	1159 vw	β-carotene
1211 w	1211 w	Tyr, Phe
1243 s	1249 m	amide III
1269 m	1274 m	amide III
1330 m	1330 m	Trp
1360 m	1360 m	Trp
1443 s	1457 s	CH_2, CH_3
1560 w	1559 w	Trp
1608 w	1609 vw	Phe, Tyr
1664 s	1663 s	amide I

from fowl body feather,[3] and found that 85% (in weight) of proteins became soluble, whereas 15% remained still insoluble. The amino acid compositions of these two categories of proteins were found to be somewhat different as shown in the last two columns of Table 1. Thus, in our analysis of the Raman spectra, we must take into account that our sample contains these two categories of proteins: "potentially CM-soluble" proteins (85%) and "potentially CM-insoluble" proteins (15%). Of course, however, all the S–S linkages as well as all the secondary structures must be intact in our sample, which is not carboxymethylated nor hydrolyzed.

From such results of the amino acid analysis, some characteristics of the feather protein could be deduced. 1) In comparison to silk fibroin,[1] for example, fowl feather contains more proline residues, which are in general abundant in β-turn structures. 2) The alanine, glycine, leucine, and valine contents are relatively low, suggesting that the β-sheet structure must be often interrupted. Such peculiarities gives an outline of a conceptual structure of the feather. By taking the fact that the feather has an anisotropic structure in situ, for which no spinning procedure is required, it is predicted that the feather must consist of a number of smaller β-sheet fragments fixed firmly along an axis through β-turns and through some other polypeptide structures.

For the proteins of the CM-soluble portion, a more detailed chemical analysis was made.[3,6,20] Here, about 69% were found to consist of relatively small and nearly homogeneous protein molecules. One such molecular component, B-4 (96 residues, 10.2 kDa) was sequenced,[6] and was predicted to have a secondary structure consisting 50% antiparallel β-sheet (Fig. 4) and

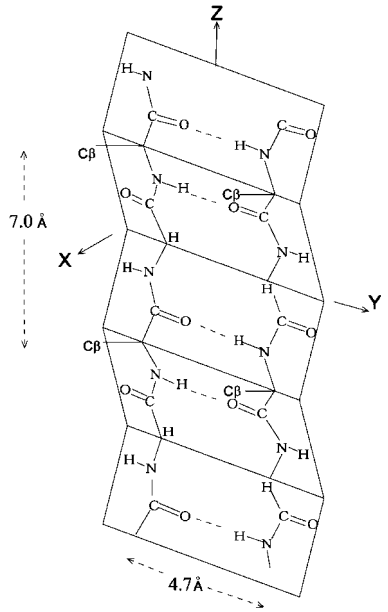

Fig. 4. Perspective drawing of an antiparallel β-sheet structure. The X, Y, and Z are the principal axes of Raman tensor of amide I band, and also of amide III band.

50% non-β-sheet (unordered chain plus β-turns). It has also been suggested that each of the two polypeptide chains per pleated-sheet segment extends for four residues and each is capped by a β-turn or turn-like structure consisting on average of four residues.[20–23] Such predictions were supported by the present Raman spectroscopic measurements, as will be detailed below.

The fowl feather rachis proteins in our sample have been found to be categorized into another set of two divisions. The solid sample (insoluble in D_2O) is not readily deuterated.[24,25] Under severe conditions (40 °C, 7 days, see Experimental), however, deuteration took place. As is seen in Fig. 2, the Raman scatterings in the 1240–1260 cm^{-1} region decreased in intensity on deuteration, and those in the 960 cm^{-1} region increased. These scatterings correspond to amide III and amide III′ bands, respectively (see Table 3), and it is evident that some of the peptide (CONH) groups of native feather proteins are converted into COND with the 40 °C–7 days D_2O action. The extent of deuteration was estimated to be $20 \pm 5\%$ from the integrated scattering intensities in the range of 1212–1300 cm^{-1}. Let us call proteins in this portion (about 20%) as "exposed proteins" and those in the remaining portion (about 80%) as "buried or rigid proteins."

Conformation of Polypeptide Main Chain. For the –CONH– group, six characteristic vibrations are known.[26] They are amide I (C=O and C–N out-of-phase stretching, around 1635–1718 cm^{-1}), amide II (N–H in-plane bending, 1458–1566 cm^{-1}), amide III (N–H in-plane bending and C–N stretching, 1247–1312 cm^{-1}), amide IV (C=O in-plane bending, 627–629 cm^{-1}), amide V (N–H out-of-plane bending, 648–790 cm^{-1}), and amide VI (C=O out-of-plane bending, 585–615 cm^{-1}). Their vibrational frequencies in some different hydrogen-bonded states are listed in the parentheses.

In a polypeptide chain, a peptide–peptide vibrational coupling takes place, and each of the frequencies given above

Table 3. Characteristic Frequencies (cm^{-1}) of Polypeptide Chains with Different Secondary Structures (from T. Miyazawa, M. Tsuboi, and others[27–37])

	α-Helix			β-Sheet				β-Turn	Random coil
	A	E_1	E_2	A	B_1	B_2	B_3		
Amide I	1652	1655	—	1667	1684	1633	—	1672	1651
Amide III	1299	1285	—	1233	1231	—		1258	1275

shows a specific splitting. In the α-helix structure of C_∞ (point group symmetry) every peptide vibration splits into A-, E_1-, and E_2-type vibrations. Whereas, in the pleated β-sheet structure of D_2 (point group symmetry), every peptide vibration splits into A-, B_1-, B_2-, and B_3-type vibrations. The characteristic frequencies of these coupled vibrations are shown[27–30] in Table 3, along with the frequencies expected for a random coil structure, where the peptide groups have no regular arrangement, and also for β-turn.[31,32]

The Raman spectrum of fowl feather rachis, as seen in Fig. 2a, shows strong bands at 1664 and 1243 cm^{-1}, and these were assigned to the A-type vibrations of amide I and III, respectively, of antiparallel β-sheet. Because no bands were seen around 1652 and 1299 cm^{-1}, no α-helical structure is considered to be involved in feather rachis. Under these β-sheet amide I and amide III band, however, β-turn and/or random coil bands are possibly hidden. It is interesting that, on deuteration, the peak at 1243 cm^{-1} disappeared and the peak at 1249 cm^{-1} remained. This fact suggests that the "exposed portion" involves more β-sheet, and the "buried portion" has more turns and/or random coils. No band assignable to the amide II, IV, V, and VI vibrations were found; they are probably too weak to be detected.

Orientation of Polypeptide Main Chain. For interpreting the polarized Raman spectra (Fig. 3), we need to have a background knowledge of the Raman tensors of the observed Raman bands. A Raman tensor ($\boldsymbol{\alpha}$), in general, connects the polarization direction of the exciting light (vector $\boldsymbol{E}$) and the polarization direction of the scattering light (vector $\boldsymbol{S}$), as $\boldsymbol{S} = \alpha \boldsymbol{E}$. The Raman tensor corresponding to a vibrational mode can be described in terms of three non-zero (principal axis) components, which are α_{xx}, α_{yy}, and α_{zz}, where xyz are coordinate axes properly defined for the tensor. Many Raman tensors have so far been determined through polarized Raman spectroscopic measurements of single crystals, whose structures are known, as well as depolarization ratio measurements of solutions.[33] In Fig. 5, some of the Raman tensors, relevant to the present structure analyses, are shown.

For amide I and amide III Raman bands of the peptide group, tensors are shown in Figs. 5a and 5b, respectively.[34] The amide I mode involves mainly stretching of the carbonyl bond. A polarized Raman spectroscopic study of the aspartame (α-L-aspartyl-L-phenylalanine methyl ester), has shown that the largest polarizability oscillation for the amide I band takes place along a line that is in the plane of the peptide group and is directed at an angle of 34° from the peptide C=O bond, as indicated in Fig. 5a. This line of largest polarizability oscillation is selected as the principal x axis of the Raman tensor. The principal y axis is also selected in the peptide plane (perpendicular to x) while the principal z axis is perpendicular to the peptide plane.

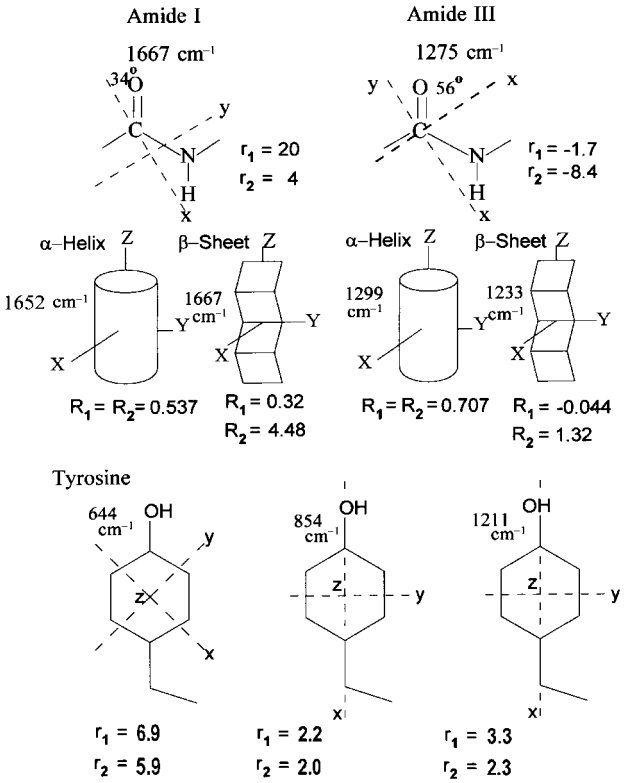

Fig. 5. Principal axes and components of Raman tensors of some normal vibrations. (a) Principal axes (x and y) and tensor values ($r_1 = \alpha_{xx}/\alpha_{zz}$ and $r_2 = \alpha_{yy}/\alpha_{zz}$) of amide I vibration of peptide. z-Axis is perpendicular to the (xy) plane. (b) x, y, z, r_1, and r_2 of the amide III vibration of peptide. (c) Principal axes (X, Y, and Z) and tensor values ($R_1 = \alpha_{XX}/\alpha_{ZZ}$ and, $R_2 = \alpha_{YY}/\alpha_{ZZ}$) of the amide I vibration of α-helix. (d) X, Y, Z, R_1, and R_2 of the amide I vibration of β-sheet. (e) X, Y, Z, R_1, and R_2 of the amide III vibration of α-helix. (f) X, Y, Z, R_1, and R_2 of the amide III vibration of β-sheet. (g) Principal axes (x, y, and z) and tensor values ($r_1 = \alpha_{xx}/\alpha_{zz}$ and $r_2 = \alpha_{yy}/\alpha_{zz}$) of three vibrations of tyrosine residues.

The amide I Raman tensor of Fig. 5a appears to be nearly unchanged when the peptide group is incorporated within a long α-helix, as demonstrate in polarized Raman studies of both polypeptide[35] and protein[36] α-helices. Using atomic coordinates given by Bamford et al.[37] for peptide N, C, and O atoms in the α-helix, the direction cosines for the principal axes defined above (xyz) in relation to a helix-fixed coordinate system (XYZ) can be calculated directly. The latter coordinate system is defined such that the Z axis is along the α-helix axis and the equivalent X and Y axes are perpendicular to Z. Using the experimental local tensor values ($r_1 = \alpha_{xx}/\alpha_{zz} = 20$) and ($r_2 = \alpha_{yy}/\alpha_{zz} = 4$), the corresponding nonlocal Raman tensor

Table 4. Raman Tensor Components and Some Related Values[a)]

	r_1	r_2	ρ		R_1	R_2	***Icc*/*Ibb***
Amide I	20	4	0.21	α-helix	0.537	0.537	3.47
				β-sheet	0.319	4.479	0.28
Amide III	−1.7	−8.4	0.35	α-helix	0.707	0.707	2.0
				β-sheet	−0.044	1.32	2.45

a) $r_1 = \alpha_{xx}/\alpha_{zz}$, $r_2 = \alpha_{yy}/\alpha_{zz}$, and $\rho =$ depolarization ratio were found for aspartame [M. Tsuboi, T. Ikeda, T. Ueda, *J. Raman Spectrosc.* **1991**, *22*, 619]. $R_1 = \alpha_{XX}/\alpha_{ZZ}$ and $R_2 = \alpha_{YY}/\alpha_{ZZ}$ for α-helix and β-sheet. Aspartame tensor is modified before it is pasted on each structure. Here, the component values are kept unchanged, and the axes are tilted so that the experimental ***Icc*/*Ibb*** is reproduced.

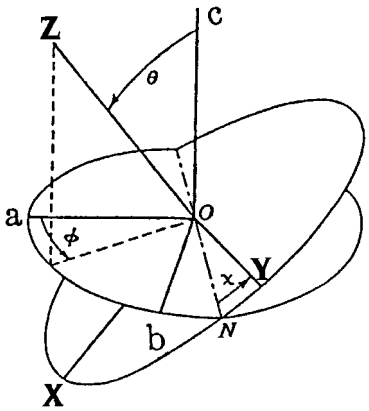

Fig. 6. Definition of the Eulerian angles, θ, χ, and ϕ, which relate the *xyz* and ***abc*** coordinate systems. Here, O–N is the line of intersection of the (*xy*) plane and (***ab***) plane. If the ***abc*** system has a cylindrical symmetry so that ***a*** and ***b*** axes are equivalent, the angle ϕ is indefinite and not significant.

values were calculated. The results, ($R_1 = \alpha_{XX}/\alpha_{ZZ} = 0.537$) and ($R_2 = \alpha_{YY}/\alpha_{ZZ} = 0.537$), are given in Table 4. In the same Table, a similar set of values, ($R_1 = \alpha_{XX}/\alpha_{ZZ} = 0.32$) and ($R_2 = \alpha_{YY}/\alpha_{ZZ} = 4.48$) are presented for nonlocal Raman tensor of pleated β-sheet on the basis of the atomic coordinates given by Pauling and Corey.[38] Here, the principal axes of the nonlocal Raman tensor of amide I of pleated β-sheet were defined such that *Z* is directed along the polypeptide chain in the plane of the sheet, *Y* was in the same plane, perpendicular to *Z* and approximately parallel to the peptide carbonyls, and *X* was perpendicular to the *YZ* plane (see Fig. 4). In Table 4, Raman tensor values of amide III of pleated β-sheet are also given, which are determined from a localized amide III tensor of CONH shown in Fig. 5b.

In many biological systems, the target proteins exhibit axial symmetry, and this is the case for fowl feather barbs, fowl feather rachis, and silks. In such cases, the ***a*** and ***b*** axes are equivalent, and only four intensity ratios, ***Ibb***, ***Icc***, ***Ibc***, and ***Iab*** are non-redundant. The orientation of the *xyz* axis system (or *XYZ* axis system) in the ***abc*** axis system is then given by the two angles θ and χ (for definition, see Fig. 6). The polarized Raman intensity quotient ***Icc*/*Ibb*** are related with θ and χ by Eq. 1:

$$\begin{aligned} \boldsymbol{Icc}/\boldsymbol{Ibb} = {} & 4[\sin^2\theta(r_1\cos^2\chi + r_2\sin^2\chi) + \cos^2\theta]^2/ \\ & [\cos^2\theta(r_1\cos^2\chi + r_2\sin^2\chi) \\ & + r_1\sin^2\chi + r_2\cos^2\chi + \sin^2\theta]^2. \end{aligned} \quad (1)$$

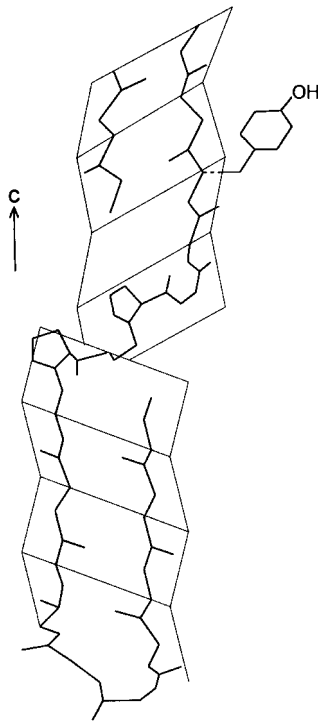

Fig. 7. Possible structures and orientations of atomic groups in fowl feather.

Inspection of the polarized Raman spectra (Fig. 3) indicates that ***Icc*** < ***Ibb*** for the bannd at 1664 cm^{-1} (amide I) and ***Icc*** > ***Ibb*** for the band at the 1243 cm^{-1} (amide III). This fact shows that the pleated β-sheets in feather are mostly aligned with its *Z* axis along the fiber axis ***c*** (Fig. 7), because the greatest polarizability oscillation of amide I mode is known to take place along the *Y* axis (Table 4, second line), and rather great polarizabilty oscillation of amide III mode along the *Z* axis. More detailed observation, however, indicates that ***Icc*/*Ibb*** = 0.48 for amide I and ***Icc*/*Ibb*** = 1.36 (Fig. 3), in contrast to the values, ***Icc*/*Ibb*** = 0.28 and ***Icc*/*Ibb*** = 2.45, found by Pézolet et al.[39] for fibroin fiber of *B. mori* silk. This fact may be taken as indicating that the silk fiber consists of polypeptide chains, which construct nearly perfect pleated β-sheet everywhere in the fiber, whereas fowl feathers have many non-β-sheet places (unordered chain plus β-turns),[20,23] beside the regular β-sheets.

A more detailed examination of the polarized Raman spectra (Fig. 8) indicates that both of the amide I and amide III regions are complex. Besides the main peaks at 1664 and

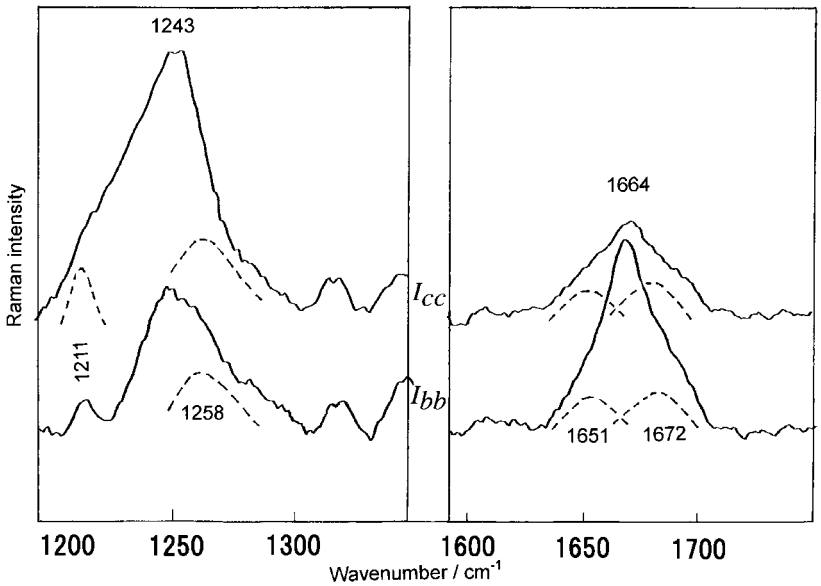

Fig. 8. Polarized Raman spectra of fowl feather rachis in the 1150–1300 and 1600–1750 cm^{-1} regions. – – –: expanded recordings.

1243 cm^{-1}, satellite bands are seen at 1672, 1651, and at 1258 cm^{-1}. These satellite scatterings are assigned to some unordered polypeptide chain,[10–12] and are thought to contribute nearly the same amounts of intensity to ***Icc*** and ***Ibb*** spectra. Curve fitting trials for a number of amide I and amide III experimental curves were made, with the assumption that $\boldsymbol{Icc}/\boldsymbol{Ibb} = 0.28$ for the band at 1664 cm^{-1} (amide I of perfect β-sheet), $\boldsymbol{Icc}/\boldsymbol{Ibb} = 2.45$ (amide III of perfect β-sheet) for the band at 1243 cm^{-1}, and $\boldsymbol{Icc}/\boldsymbol{Ibb} = 1$ for the non-β-sheet bands at 1672, 1651, and 1258 cm^{-1}. The results indicate that $65 \pm 10\%$ of the feather rachis peptide chains are nearly perfect β-sheets and $35 \pm 10\%$ are unordered polypeptide chains including β-turns. On the basis of an amino acid sequences, a model of the polypeptide chain in the fowl feather rachis has been previously proposed.[20] It consists of relatively short polypeptide chains (such as B-4, which is like a rectangular block[1] of $9.7 \times 4.7 \times 4.7$ Å^3), that are connected through chains involving proline residues. Such a model, redrawn in Fig. 7, is consistent with our present experimental results just described.

Tyrosine Residues. About 1.3 tyrosine residues per 100 residue-unit (e.g., B-4) give rise to a Raman band at 644 cm^{-1} (see Figs. 2 and 3). This band has been assigned to a vibration of the *para*-phenoxy ring, which is similar in nature to the mode of benzene occurring at 605 cm^{-1}.[40,41] The Raman tensor of the band at 644 cm^{-1} band has principal axis x and y that are rotated by 45° from the line intersecting the C^{γ} and C^{ζ} atoms (see lower-left corner of Fig. 5). The tensor quotients r_1 ($\equiv \alpha_{xx}/\alpha_{zz}$) and r_2 ($\equiv \alpha_{yy}/\alpha_{zz}$) have values of 6.9 and −5.9, respectively.[42] The large tensor ratios and significant polarization observed for this band ($\boldsymbol{Icc}/\boldsymbol{Ibb} = 1.6$, see Fig. 3) are favorable for gaining information about the average phenoxy ring orientation for tyrosine residues.

The strong Raman band at 854 cm^{-1} (Fig. 3) is well-known to be due to the phenoxy ring breathing vibration. The Raman tensor is known to be relatively isotropic with respect to the in-plane components (α_{xx} and α_{yy}), but the out-of-plane component α_{zz} differs greatly from α_{xx} or α_{yy} (Fig. 5, lower-center).[42] Accordingly, the large polarization that was observed provides strong evidence that the phenoxy ring planes cannot all be perpendicular to the fiber axis (***c***-axis).

The weak, but well-resolved, Raman band at 1211 cm^{-1} in Fig. 2 is also assignable to the feather rachis tyrosines. In the spectrum of the L-tyrosine crystal, the corresponding band, which occurs at 1200 cm^{-1}, has been assigned to a vibration involving predominantly the stretching of C^{β}–C^{γ} bond.[42] From ab initio calculation determines the wavenumber value for this mode has been determined to be 1209 cm^{-1} and it has been shown that the polarizability oscillation is greatest along the C^{β}–C^{γ} bond.[42] Experimental data obtained on an oriented L-tyrosine single crystal indicate the polarized Raman spectrum (***Ibb***) is most intense when the crystallographic b-axis is parallel to the C^{β}–C^{γ} bond, consistent with the ab intio calculations.[42] For the band at 1211 cm^{-1} of feather rachis, ***Icc*** was observed to be greater than ***Ibb*** (Fig. 8). This causes an anticipation that the tyrosyl C^{β}–C^{γ} bond direction is rather parallel, not perpendicular, to the fiber axis of feather. A more precise orientation (θ and χ in Fig. 6) is given below through Eq. 1.

For the band at 854 cm^{-1}, it was found that $\boldsymbol{Icc}/\boldsymbol{Ibb} = 1.8$ (by the use of several expanded recordings, by drawing the baselines, and by subtracting the skirts of the band at 830 cm^{-1}). By applying this value to Eq. 1 and with the known r_1 and r_2 values (Fig. 5), a contour line in (θ, χ) space was obtained, Fig. 9. Similarly, Figure 9 shows the contour line obtained for the band at 1211 cm^{-1} ($\boldsymbol{Icc}/\boldsymbol{Ibb} = 2.0$, with r_1 and r_2 values also as given in Fig. 5). Finally, the corresponding data for the band at 644 cm^{-1} ($\boldsymbol{Icc}/\boldsymbol{Ibb} = 1.6$, with r_1 and r_2 values given in Fig. 5) yield the contour line that is plotted on the same (θ, χ) coordinate system as that in Fig. 9 after accounting for the required 45° rotation about the z-axis. The intersection of the three contour lines represents the region of (θ, χ) that corresponds to the average phenolic ring orientation of the tyrosine, i.e., $\theta = 70 \pm 10°$ and $\chi = 24 \pm 10°$. This average orientation of tyrosine residues is shown in Fig. 7.

The present Raman spectra of feather rachis indicates another aspect of the tyrosine residues, i.e., their hydrogen-bonding

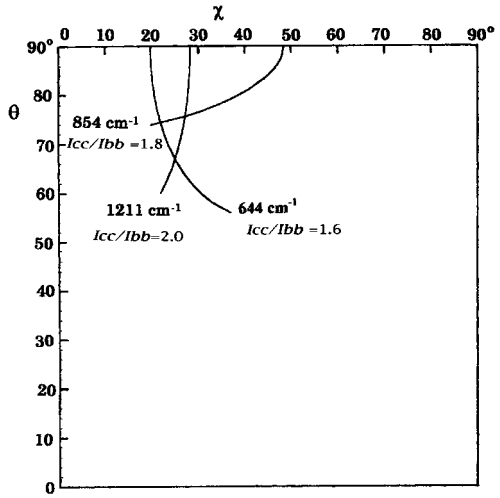

Fig. 9. Contour plots in (θ, χ) space of the polarized Raman intensity ratios ***Icc/Ibb*** of the tyrosine marker bands at 644, 854, and 1211 cm^{-1} in the spectrum of fowl feather rachis. The plots were obtained from Eq. 1 using the known r_1 and r_2 values given in Fig. 5.

states. Tyrosine shows a Raman band at 830 cm^{-1} besides the strong band at 854 cm^{-1} (Figs. 2 and 3). It is now known that 845/830 cm^{-1} is a Fermi-resonance doublet and that the $I(845)/I(830)$ intensity ratio is 0.30 when the tyrosine phenoxyl proton is a strong hydrogen-bond donor, and when the tyrosine phenoxy oxygen is a strong hydrogen-bond acceptor $I(845)/I(830) = 2.5$.[40] If the phenoxy group acts as both a donor and an acceptor of hydrogen bonds, as is expected for a solvent-exposed tyrosine, then $I(854)/I(830)$ is approximately 1.25.[40]

In the absence of hydrogen bonding, the Raman intensity of the higher-wavenumber component of the canonical Fermi doublet is greatly enhanced ($I(845)/I(830) = 6.7$).[43] Thus, the tyrosines in feather rachis are considered to have phenoxy oxygens acting as strong hydrogen-bond acceptors, but the phenoxy protons are not acting as hydrogen-bond donors, because the $I(854)/I(830)$ here was found to be about 2.0 (Fig. 3).

Phenylalanine Residues. About three phenylalanine residues are involved in fowl feather rachis (per 100 amino acid residues), and they generate prominent phenyl ring markers at 623, 1003, and 1033 cm^{-1} (Figs. 2 and 3). The intensity ratios ***Icc/Ibb*** were found to be nearly one for all three bands (Fig. 3). This fact may be taken as indicating that the phenyl rings of phenylalanines have no preferable orientation in the fiber so that their directions are randomly distributed. It is not plausible that every tensor of these three bands has a special orientation, which happens to cause $\boldsymbol{Icc/Ibb} = 1$.

Tryptophan Residues. There is only one tryptophan residue per two 100-residue units of fowl feather rachis. In addition, it is involved only in the insoluble portion, and none of it is found in the soluble portion that has been better characterized chemically. Therefore, one might be inclined to ignore a possible significance of its existence. It is interesting, however, that it gives prominent Raman bands at 760, 1330, 1360, and 1560 cm^{-1}, and a definite scattering anisotropy (Figs. 2 and 3).

Icc/Ibb of the tryptophan markers at 1330 (W7′ mode), 1360 (W7), and 1560 cm^{-1} (W3) were found to be 0.91, 0.67, and 0.78, respectively (Fig. 3). From this set of data, the specific geometric parameters (θ and χ) can be determined using the Raman tensors (Table 5) previously determined.[44] The procedure was similar to that for the determination of the tyrosine orientation. In other words, we substituted the experimental value of ***Icc/Ibb*** and Raman tensors of the band at 1330 cm^{-1} into Eq. 1 to find the set of (θ, χ) values consistent with the data. This set defines a contour line of constant intensity ratio in (θ, χ) space. The same procedure yields contour lines in (θ, χ) space for the band at 1360 and 1560 cm^{-1}. From the intersections of the three contour lines, we obtained $\theta = 37.5 \pm 5.0^\circ$ and $\chi = 47.5 \pm 10.0^\circ$. It is noticeable that the tryptophan indolyl ring is located rather flat (rather perpendicular than parallel, $\theta = 38^\circ$) to the fiber axis, in contrast to the tyrosine phenoxyl ring which is more or less parallel ($\theta = 70^\circ$) to the fiber axis.

Cystine Linkages. Feather rachis has about 8 cysteine residues per 100 amino acid residues (Table 1), and thus about four S–S linkages. The Raman bands in the 510–540 cm^{-1} region are assignable to the S–S stretching vibrations. As are seen in Fig. 2, two Raman peaks are found in this region at 513 and 525 cm^{-1}. On the basis of an extensive study of Sugeta et al.[45] on the vibrations of a number of dialkyl disulfide molecules, the 513 cm^{-1} Raman band was attributed to a structure, in which both of the C^{α}–C^{β}–S–S portions around the cystine linkage have *gauche* conformations, whereas the 525

Table 5. Raman Tensors of Selected Bands of the Tryptophan Side Chain[a)]

Band/cm^{-1}	Mode	r_1 ($\equiv\alpha_{xx}/\alpha_{zz}$)	r_2 ($\equiv\alpha_{yy}/\alpha_{zz}$)	Principal axes
1330	W7′	2.26	0.35	y: intersects $C^{\zeta 3}$ and $C^{\delta 2}$ x: ⊥ to y and intersects $C^{\zeta 2}$ z: ⊥ to y and x
1360	W7	1.56	6.13	y: intersects $C^{\varepsilon 3}$ and $C^{\delta 1}$ x: ⊥ to y and intersects $C^{\zeta 2}$ z: ⊥ to y and x
1560	W3	0.59	2.71	y: intersects $C^{\zeta 3}$ and $C^{\delta 2}$ x: ⊥ to y and intersects $C^{\zeta 2}$ z: ⊥ to y and x

a) Determined from polarized Raman analysis of a single crystal of *N*-acetyl-L-tryptophan (Tsuboi et al. 1996[44]).

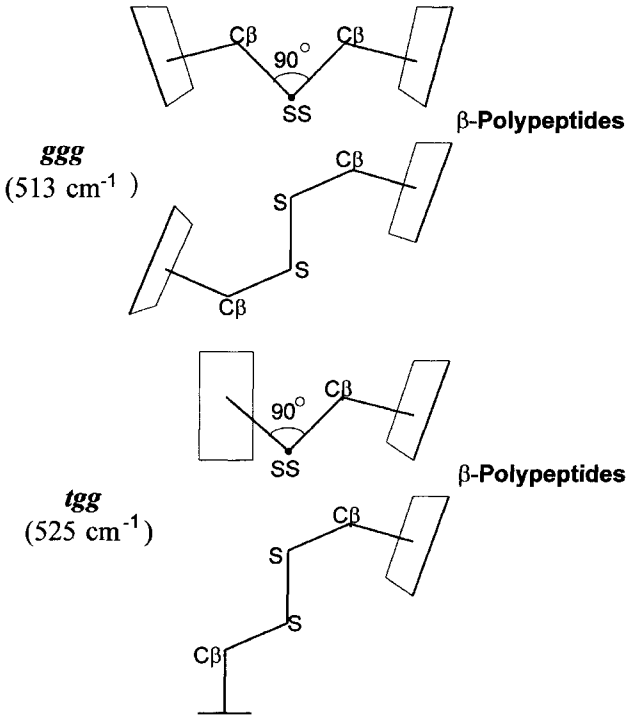

Fig. 10. The possible –S–S– linkages *ggg* and *tgg* involved in feather rachis structure. In each of the presentations of these two forms, the upper portion shows the view along the S–S bond direction, and the lower portion the view along a perpendicular direction to the S–S bond.

cm^{-1} band was attributed, to a structure, in which one of the two C^{β}–S bonds in the C^{α}–C^{β}–S–S–C^{β}–C^{α} linkage is in a *trans* and the other a *gauche* conformation.

The internal rotation angle around the S–S bond as axis is considered to be 90°, on the basis of its electronic structure and on the basis of various examples in the protein structures (Protein Databank). By considering this as nearly gauche, the former (with the band at $513\,cm^{-1}$) has a *ggg* conformation and the latter (with the band at $525\,cm^{-1}$) has a *tgg* conformation. These two conformations are illustrated in Fig. 10. As may be seen here, the *ggg* cystine can connect two β-polypeptides that are nearly parallel to each other. On the other hand, the *tgg* cystine can connect two β-polypeptides that are nearly perpendicular to each other. The abundance ratio of the *ggg* versus *tgg* cystins was estimated to be about 2:1 from the intensity ratio in the Raman spectrum (Fig. 2).

It may seem peculiar that, on the partial deuteration, the Raman bands at 513 and $525\,cm^{-1}$ were replaced by a stronger and broader one peak at $517\,cm^{-1}$ (see Fig. 2). It is speculated that this is caused by an overlap of the peptide V′ band (N–D out-of-plane bending vibration), and that even a partially deuterated feather has two cystine likages (*ggg* and *tgg*).

The ***Ibb*** of the band at $513\,cm^{-1}$ was slightly, but noticeably, greater than ***Icc*** (Fig. 3). Also, the higher frequency shoulder (probably unresolved $525\,cm^{-1}$ band) was more prominent for ***Ibb*** than for ***Icc***. These facts suggest that the S–S bonds are directed slightly more frequently in lateral directions ($\perp$ ***c***-axis) rather than along the longitudinal direction ($\parallel$ ***c***-axis).

Conclusion

The solid-state fowl feather rachis consists of about 65% antiparallel polypeptide chain pleated sheets. Every sheet is rather small, something like 9.7×4.7 Å, (two antiparallel polypeptide chains each of which has about four amino acid residues), and the sheets are connected covalently through randomly oriented polypeptide chains and β-turns ($\approx$35%) to form a molecule of about 100 amino acid residues. Each sheet is oriented with its long axes (*Z*-axis, see Fig. 4) along the feather ***c***-axis, but its *X*- and *Y*-axes oriented randomly in the feather ***ab*** plane (see Fig. 7). Each sheet is connected with another sheet running parallel through a *ggg* cystine and with that running perpendicularly through a *tgg* cystine. Here, *ggg* was shown to be two times more abundant than the *tgg* cystine. Every about two sheets has one tyrosine side chain stuck out with the phenoxyl plane inclined by about 20 degrees from the fiber axis ***c***. Phenylalanine side chain (one for every sheet in an average) seems to take random orientation, while tryptophan indole ring buried in the insoluble core is located with its plane rather flat (inclination = 38°) in the ***ab*** plane of the feather.

References

1 R. D. B. Fraser, T. P. MacRea, *Conformation in Fibrous Proteins and Related Synthetic Polypeptides*, Academic Press, New York, **1973**.

2 A. M. Woodin, *Nature* **1954**, *173*, 823.

3 K. Akahane, S. Murozono, K. Murayama, *J. Biochem. (Tokyo)* **1977**, *81*, 11.

4 A. Murayama, K. Akahane, S. Murozono, *J. Biochem. (Tokyo)* **1977**, *81*, 19.

5 S. Murozono, K. Murayama, K. Akahane, *J. Biochem. (Tokyo)* **1977**, *81*, 53.

6 K. M. Arai, R. Takahashi, Y. Yokote, K. Akahane, *Eur. J. Biochem.* **1983**, *132*, 501.

7 K. M. Arai, R. Takahashi, Y. Yokote, K. Akahane, *Biochim. Biophys. Acta* **1986**, *873*, 6.

8 A. T. Tu, *Spectroscopy of Biological Systems, Advances in Spectroscopy*, ed. by R. J. Clark, R. E. Hester, Wiley, Chichester, **1986**, Vol. 13, pp. 47–112.

9 I. Harada, H. Takeuchi, *Spectroscopy of Biological Systems, Advances in Spectroscopy*, ed. by R. J. Clark, R. E. Hester, Wiley, Chichester, **1986**, Vol. 13, pp. 113–175.

10 G. J. Thomas, Jr., B. Prescott, *Biopolymers* **1987**, *26*, 921.

11 T. Miura, G. J. Thomas, Jr., *Introduction to Biophysical Methods for Protein and Nucleic Acid Research*, Academic Press Inc., London, **1995**, pp. 261–315.

12 T. Miura, G. J. Thomas, Jr., *Subcellular Biochemistry*, Plenum Press, New York, NY, **1995**, pp. 55–99.

13 S. A. Overman, G. J. Thomas, Jr., *Biochemistry* **1998**, *37*, 5654.

14 M. Tsuboi, S. A. Overman, G. J. Thomas, Jr., *Biochemistry* **1996**, *35*, 10403.

15 M. Tsuboi, K. Ushizawa, K. Nakamura, J. M. Benevides, S. A. Overman, G. J. Thomas, Jr., *Biochemistry* **2001**, *40*, 1238.

16 M. Tsuboi, J. M. Benevides, B. Priya, G. J. Thomas, Jr., *Biochemistry* **2005**, *44*, 4861.

17 W. A. Schroeder, L. M. Kay, B. Lewis, N. Hunger, *J. Am. Chem. Soc.* **1955**, *77*, 3901.

18 B. Penke, R. Ferenczi, K. Kovacs, *Anal. Biochem.* **1974**,

60, 45.
19 B. S. Harrap, E. F. Woods, *Biochem. J.* **1964**, *92*, 8.
20 Y. Takahashi, K. M. Arai, Y. Yokote, K. Akahane, *Sci. Bull. Josai Univ.* **1993**, *1*, 31.
21 P. Y. Chou, G. D. Fasman, *Annu. Rev. Biochem.* **1978**, *47*, 251.
22 J. Garnier, D. J. Osguthorpe, B. Robson, *J. Mol. Biol.* **1978**, *120*, 97.
23 S. L. Hsu, W. H. Moore, S. Krimm, *Biopolymers* **1976**, *15*, 1513.
24 K. D. Parker, *Biochim. Biophys. Acta* **1955**, *17*, 148.
25 R. D. B. Fraser, T. P. MacRea, *J. Chem. Phys.* **1958**, *29*, 1024.
26 T. Miyazawa, T. Shimanouchi, S. Mizushima, *J. Chem. Phys.* **1956**, *24*, 408.
27 T. Miyazawa, *J. Chem. Phys.* **1960**, *32*, 1647.
28 M. Tsuboi, F. Kaneuchi, T. Ikeda, K. Akahane, *Can. J. Chem.* **1991**, *69*, 1752.
29 M. Tsuboi, A. Wada, *J. Mol. Biol.* **1961**, *3*, 480.
30 T. Miyazawa, E. Blout, *J. Am. Chem. Soc.* **1961**, *83*, 712.
31 G. J. Thomas, Jr., B. Prescott, D. W. Urry, *Biopolymers* **1987**, *26*, 921.
32 B. Prescott, V. Reugopalakrishnan, G. J. Thomas, Jr., *Biopolymers* **1987**, *26*, 934.
33 M. Tsuboi, G. J. Thomas, Jr., *Appl. Spectrosc. Rev.* **1997**, *32*, 263.
34 M. Tsuboi, T. Ikeda, T. Ueda, *J. Raman Spectrosc.* **1991**, *22*, 619.
35 W. T. Wilser, D. B. Fitchen, *J. Chem. Phys.* **1975**, *62*, 720.
36 S. A. Overman, M. Tsuboi, G. J. Thomas, Jr., *J. Mol. Biol.* **1996**, *259*, 331.
37 C. H. Bamford, A. Elliott, W. E. Hanby, *Synthetic Polypeptides*, Academic Press, New York, **1956**, p. 124.
38 L. Pauling, R. B. Corey, *Proc. Natl. Acad. Sci. U.S.A.* **1953**, *39*, 253.
39 M.-E. Rousseau, T. Lefèvre, L. Beaulieu, T. Asakura, M. Pézolet, *Biomacromolecules* **2004**, *5*, 2247.
40 M. N. Siamwiza, R. C. Lord, M. C. Chen, T. Takamatsu, I. Harada, H. Matsuura, T. Shimanouchi, *Biochemistry* **1975**, *14*, 4870.
41 H. Takeuchi, N. Watanabe, I. Harada, *Spectrochim. Acta, Part A* **1988**, *44*, 74.
42 M. Tsuboi, Y. Ezaki, M. Aida, M. Suzuki, A. Yimit, K. Ushizawa, T. Ueda, *Biospectroscopy* **1998**, *4*, 61.
43 Z. Arp, D. Autrey, J. Laane, S. A. Overman, G. J. Thomas, Jr., *Biochemistry* **2001**, *40*, 2522.
44 M. Tsuboi, T. Ueda, K. Ushizawa, Y. Esaki, S. A. Overman, G. J. Thoma, Jr., *J. Mol. Struct.* **1996**, *379*, 43.
45 H. Sugeta, A. Go, T. Miyazawa, *Bull. Chem. Soc. Jpn.* **1973**, *46*, 3407.